12th Brazilian Congress of Manufacturing Engineering
May 10th-12th, 2023, Brasilia, DF, Brazil

INFLUENCE OF INFILL DENSITY AND LAYER THICKNESS PARAMETERS ON THE MECHANICAL AND DIMENSIONAL PROPERTIES OF LOW-DENSITY PLA

Fernando Fonseca de Freitas
Hélio de Assis Pegado
Universidade Federal de Minas Gerais – Av. Pres. Antônio Carlos, 6627 – Pampulha, Belo Horizonte – MG
prosoad@gmail.com, helio@demec.ufmg.br

Abstract. *The increase in additive manufacturing (AM) in recent years has encouraged the growth of research related to the materials used in this methodology. AM uses the overlapping of consecutive layers to form an object previously designed in CAD. Polymers play an important role in this scenario. As it is a material that does not require heating the printing table and can be used with the printer open, Polylactic acid (PLA) is a very convenient polymer in the AM universe. As different projects were demanding different properties of materials, studies around the alteration of these inputs were evolving. Several works evaluating the mixture of additives to a PLA matrix are being developed in the literature. A low-density PLA was recently introduced to the AM market. This material has a foaming ability that can be controlled from the temperature setting of the 3D printer's extrusion nozzle. The present work characterizes the strength of this material and investigates the influence of two parameters, layer thickness and filling percentage, on its mechanical and dimensional properties. Specimens were printed respecting the dimensions proposed by ASTM D638. 54 specimens were separated into 3 groups of 18, whose filling percentages are 25%, 50% and 75%. Within these groups, there is a separation of 3 sets of 6 bodies with layer thicknesses of 0.12mm, 0.16mm and 0.2mm. After making the specimens, they were measured in length, width and thickness. The data from the tests and measurements were submitted to an analysis of variance, to establish, or not, a relationship between the parameters studied and the mechanical and dimensional properties of the specimens. Preliminarily, it was possible to observe the influence of the parameters of layer thickness and filling percentage on the strength of the material and the width of the specimens. On the other hand, none of these parameters affects the length of the specimen. The thickness of the specimen is only influenced by the layer thickness parameter. Considering the recent introduction of this type of PLA in the AM market, it is expected to obtain, after this work, information on the mechanical and dimensional properties necessary for mechanical projects.*
Keywords: *FDM Process; PLA; Tensile Strength; Layer Thickness; Infill Density.*

1. INTRODUCTION

Additive manufacturing (AM) technology has experienced a considerable increase in recent years (Ceulemans et. al., 2020; Chacón et al., 2017; Durakovic, 2018). AM is the technique of material deposition layer by layer that respects a model designed in Computer-Aided Design (CAD) (Goh et al., 2017; Srinivasan et al., 2020), linking the digital and the real. Several areas have increased the use of this manufacturing process over the years, such as the medical, energy and transport areas (Ceulemans et. al., 2020). The characteristics of the part created by additive manufacturing will vary depending on the process used in fabrication. Some well-known processes are Fused Deposition Modeling (FDM), Selective Laser Sintering (SLS) and Stereolithography (SLA) (Kafle et al., 2021). The FDM process consists of melting the material at the high temperature of the printing nozzle and depositing it, layer by layer, on the printing bed to form the desired design (Kafle et al., 2021). An advantage of this process is the fabrication of functional models and the easy removal of supports when compared to other AM methods (Srinivasan et al., 2020). Several parameters influence the mechanical properties of models when made by the FDM process, namely: extruder nozzle diameter, model geometry, layer thickness, material viscosity, infill pattern and infill density (Srinivasan et al., 2020).

The materials used in AM constitute an important field of study. Polymers are types of materials widely used in AM, the most commonly used are Polylactic Acid (PLA), Acrylonitrile Butadiene Styrene (ABS) and Polyethylene terephthalate glycol (PETG). The use of these materials within AM has been explored by several authors (Alghamdi et al., 2021; Castelo Branco et al., 2021; Cho et al., 2019; Cobos et al., 2019; Hanon et al., 2019, 2020, 2021; Kuznetsov et al., 2018; Moradi et al., 2021; Srinivasan et al., 2020). Studies seeking the improvement of polymeric materials have also been developed. Looking for the reduction of the structural weight works experimenting with the foaming of PLA by different methods were developed (Nofar & Park, 2014; Standau et al., 2019). Currently, there are filaments commercialized at reasonable prices.

The investigation of the influence of printing parameters on the use of PLA has already been developed by several authors. Cho et al. (2019) showed that the layer thickness has a greater influence on the mechanical properties than the infill pattern, and also that the greater the layer thickness, the greater the mechanical strength. Branco et al. (2021)

presented results that indicate that the increase in infill density, increases the mechanical strength. This characteristic agrees with the experiments carried out by Hanon et al. (2020).

Some works are studying the influence of printing parameters on the accuracy of the dimensions of the printed parts in PLA.

Hanon et al. (2021) concluded that commercial printers presented an accuracy of up to 98.81% concerning the nominal design dimensions. In addition, he observed that cylindrical specimens presented more accurate values for diameter and length. Regarding the dimensional accuracy of 3D parts for medical applications, Gendviliene et al. (2020) found that there were differences in print accuracy when comparing printers from different manufacturers. Another conclusion of their work was that morphological properties can be better achieved when different techniques are combined.

The eSUN company has developed a low-weight PLA (ePLA-LW) intended for use in drones. This material has a foaming rate that can be controlled according to the temperature of the print nozzle. The filament is introduced in a high-pressure chamber, where blowing agents, commonly CO2 and N2, are inserted into the PLA polymeric matrix. When the filament is being extruded from the nozzle these blowing agent cells nucleate and grow, creating voids within the structure, hence the name “foaming”. This procedure can be controlled by the temperature of the extrusion nozzle. Naturally, parts created from this material have a lower density. Temperatures between 190°C and 210°C do not show foam formation, according to the manufacturer the material behaves like normal PLA. The foaming gradually increases between temperatures of 210°C and 270°C (ESUN, 2022). Regarding its recent introduction in the AM market, it is necessary to characterize this material in different printing parameters. The present study intends to evaluate the influence of the infill density and layer thickness parameters on the mechanical strength of the ePLA-LW and also on the variations in length, width and thickness of the printed specimens. Considering that foaming occurs after a temperature of 210°C, and the temperature of the tests in this work was 200°C, the material strength will also be compared with works in the literature.

2. MATERIAL AND METHODOLOGY

The experimental procedures carried out in this work include characterization of the filament, fabrication of specimens, process parameters, tensile tests, measurement of dimensions and analysis of variance.

2.1 Filament characteristics

The fabrication of the specimens was done using the ePLA-LW manufactured by eSUN. Its characteristics, according to the manufacturer's website (ESUN, 2022), are:

- Density at 200°C: 1.2 g/cm³
- Filament diameter: 1.75 mm

The set temperatures were:

- Nozzle: 200°C
- Printing bed: 60°C

2.2 Specimens fabrication

The specimen was designed using the SOLIDWORKS 2018 software. After the design was completed, the model was exported in STL format. Creality Cura 4.13.0 (*Ultimaker Cura: Powerful, Easy-to-Use 3D Printing Software*, n.d.) slicing software was used to determine the print parameters (Table 1) and slice the specimen in layers. At the end of slicing, the program exports the model in a file in G-code format. The Ultimaker Ender 3 3D printer (Figure 1) reads this file from a memory card to print the designed model. 54 specimens, whose design respected the standards of ASTM D638 Type IV (Figure 2), were made.

Table 1. Print parameters

Parameters	
First layer thickness	0.2 mm
Thickness of other layers	0.12 mm - 0.16 mm - 0.2 mm
Infill density	25% - 50% -75%
Infill pattern	Triangular
Nozzle diameter	0.4 mm

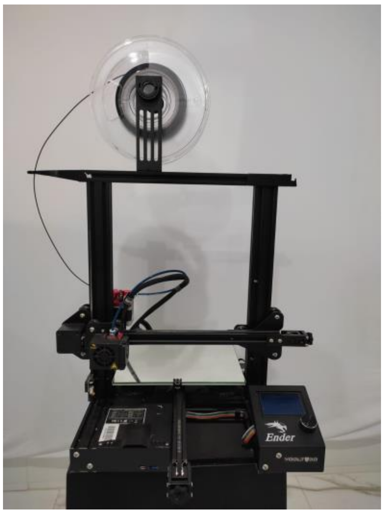

Figure 1. Creality Ender 3

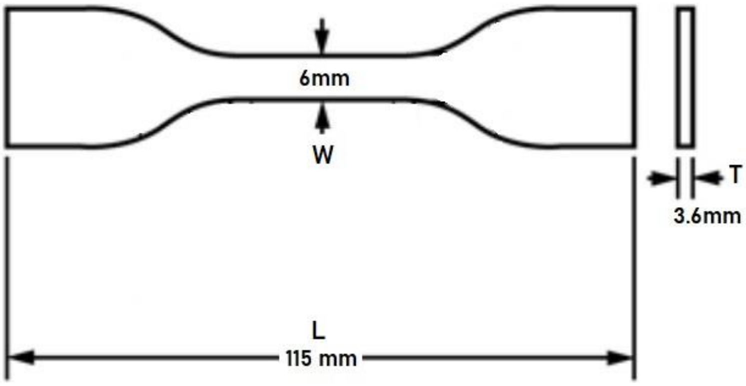

Figure 2. ASTM D638 Type IV specimen

2.3 Process parameters

The parameters studied in this work were the infill density and layer thickness. 18 specimens were made for each of the infill densities: 25%, 50% and 75% (Figure 3). For each infill value, there are 6 specimens with layer thicknesses of 0.12 mm, 0.16 mm and 0.20 mm (Figure 4).

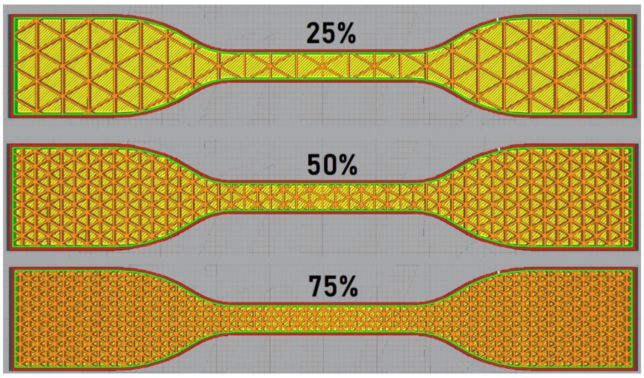

Figure 3. Infill density

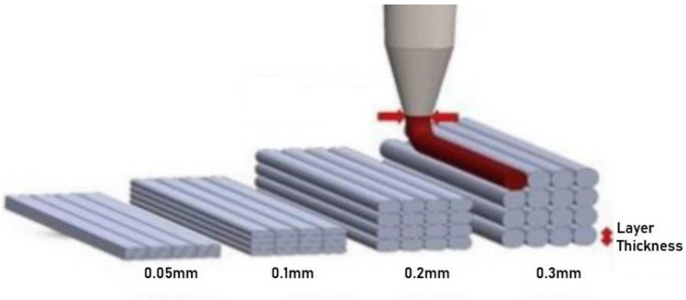

Figure 4. Layer Thickness Modified (Ayrilmis, 2018)

2.3.1 Infill density

The infill density is the amount of material deposited inside the specimen. The greater the amount of material deposited, the longer the time to print and the waste of filament.

2.3.2 Layer thickness

Layer thicknesses can be configured in the slicing software. Models with thinner layers have a better finish, but also require a longer printing time.

2.3.3 Infill pattern

Different patterns can be used as infill, such as triangular, concentric, linear, grid, etc.. The infill pattern used was triangular.

2.4 Tensile tests

The data acquisition time was set to 300/min and the speed was 50 mm/min. In total, 54 specimens were submitted to the tensile test (Figure 5). The point of the maximum ultimate tensile strength (UTS) is computed so that the influence of the parameters on this property can be examined. For the tensile tests, a universal testing machine of the Oswaldo Filizola BME-20kN model was used.

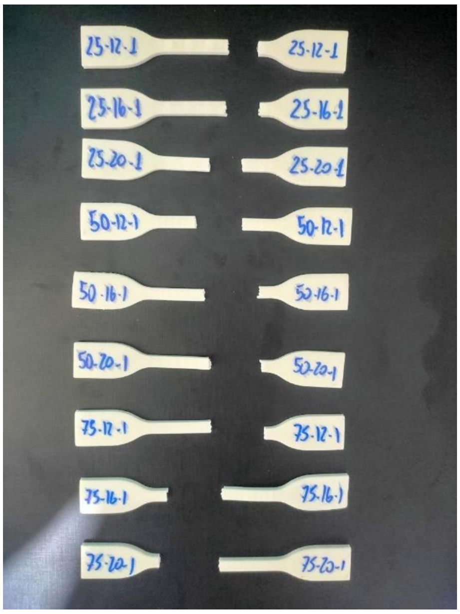

Figure 5. Specimens after tensile tests

2.5 Dimension measurement

A calliper was used to measure all 54 specimens. The dimensions referring to the length (L), width (W) and thickness (T) of the specimen were measured.

2.6 Analysis of variance

A 2-way ANOVA can be used to investigate the effects of factors A and B and the AB interaction of these factors (Montgomery & Runger, 2018). Considering **a** levels of factor **A** and **b** levels of factor **B** and **n** observations of each interaction between levels, the following table (Table 2) can be set up:

Table 2. Factor table

Factor B / Factor A	1	2	...	b	Totals	Averages
1	$x_{111}, x_{112}, \ldots, x_{11n}$	$x_{121}, x_{122}, \ldots, x_{12n}$		$x_{1b1}, x_{1b2}, \ldots, x_{1bn}$	$x_{1..}$	$\bar{x}_{1..}$
2	$x_{211}, x_{212}, \ldots, x_{21n}$	$x_{221}, x_{222}, \ldots, x_{22n}$		$x_{2b1}, x_{2b2}, \ldots, x_{2bn}$	$x_{1..}$	$\bar{x}_{1..}$
⋮					⋮	⋮
a	$x_{a11}, x_{a12}, \ldots, x_{a1n}$	$x_{a21}, x_{a22}, \ldots, x_{a2n}$		$x_{ab1}, x_{ab2}, \ldots, x_{abn}$	$x_{a..}$	$\bar{x}_{a..}$
Totals	$x_{.1.}$	$x_{.2.}$		$x_{.b.}$	$x_{...}$	
Averages	$\bar{x}_{.1.}$	$\bar{x}_{.2.}$		$\bar{x}_{.b.}$		$\bar{x}_{...}$

The null hypothesis determines that there is no significant difference between the data collected between the levels or factors. These differences are analyzed from the variances of the collected data in relation to the means within each level and factor.

The ANOVA table (Table 3) contains the source, sum of squares (SQ), degrees of freedom (DF), mean square (MQ) and F:

Table 3. ANOVA Table

ANOVA

Source	*SQ*	*DF*	*MQ*	*F*
Factor A	$SQ_A = bn\sum_{i=1}^{a}(\bar{x}_{i..} - \bar{x}_{...})^2$	$DF_A = a - 1$	$MQ_A = \frac{SQ_A}{DF_A}$	$F = \frac{MQ_A}{MQ_E}$
Factor B	$SQ_B = an\sum_{j=1}^{b}(\bar{x}_{.j.} - \bar{x}_{...})^2$	$DF_B = b - 1$	$MQ_B = \frac{SQ_B}{DF_B}$	$F = \frac{MQ_B}{MQ_E}$
Factors interaction	$SQ_{AB} = n\sum_{i=1}^{a}\sum_{j=1}^{b}(\bar{x}_{ij.} - \bar{x}_{i..} - \bar{x}_{.j.} + \bar{x}_{...})$	$DF_{AB} = (a-1)(b-1)$	$MQ_{AB} = \frac{SQ_{AB}}{DF_{AB}}$	$F = \frac{MQ_{AB}}{MQ_E}$
Error	$SQ_E = \sum_{i=1}^{a}\sum_{j=1}^{b}\sum_{k=1}^{n}(x_{ijk} - \bar{x}_{ij.})^2$	$DF_E = ab(n-1)$	$MQ_E = \frac{SQ_E}{DF_E}$	
Total	$SQ_T = SQ_A + SQ_B + SQ_R + SQ_E$	$DF_T = abn - 1$		

The null hypothesis is rejected if the calculated value of F is greater than the critical F (a function of significance and degrees of freedom) shown in Fisher's F value table. The rejection of the null hypothesis implies that there is a significant difference among the levels.

In this work there are 2 factors (layer thickness and fill density) and 3 levels in each of these factors: 0.12 mm, 0.16 mm and 0.2 mm for the layer thickness factor and 25%, 50% and 75% for the infill density factor. Six tests were performed for each factor-level configuration.

3. RESULTS AND DISCUSSION

3.1 Ultimate tensile strength

The average values of the UTS of the 6 specimens for each layer thickness and infill density are shown in Figure 6. The results suggest that the lowest resistance limits are from specimens whose parameters were 0.12 mm thickness and 25% infill. The highest average values of resistance are from specimens of 75% infill and 0.16 mm layer thickness. It can also be inferred that the higher the infill density, the greater the resistance. The resistances of 0.16mm and 0.2mm are the same, considering the error involved.

For a layer thickness of 0.15 mm, Pandzic et. al. (2019) found results of 16.5 MPa, 19.3 MPa and 21.4 MPa for infill densities of 20%, 50% and 70%, respectively. Fernandes (n.d.) found values of 20.2 MPa and 17.67 MPa for a filling density of 20% and a layer thickness of 0.1 mm and 0.2 mm. In the same work, values of 19.91 MPa and 22.24 MPa, respectively, were found for 40% filling and layer thickness of 0.1 mm and 0.2 mm. Likewise, for the value of 60% filling and layer thicknesses of 0.1 mm and 0.2 mm, the tensile strength values were 29.43 MPa and 25.22 MPa.

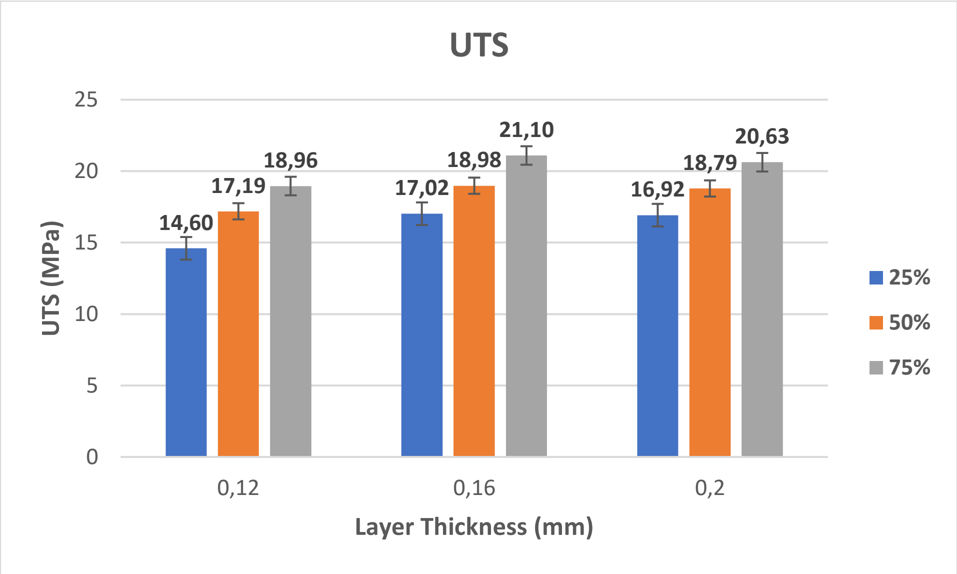

Figure 6. Graph plotted UTS by layer thickness for 25%, 50% and 75% infill respectively

From the ANOVA (Table 4), it is observed that both layer thickness and the infill density F values are greater than the critical F. Thus, the null hypothesis is rejected. Therefore, both parameters are factors that impact the UTS of the specimen.

Table 4. UTS

Source	*SQ*	*DF*	*MQ*	*F*	*Critical F*
Layer thickness	48.08051	2	24.04025	46.538	5.110318
Infill density	147.491	2	73.74552	142.7593	5.110318
Factors interaction	1.190384	4	0.297596	0.576097	3.767427
Error	23.245106	45	0.516558		
Total	220.0077	53			

3.2 Specimens dimensions

3.2.1 Length

The maximum and minimum absolute errors were 0.38 mm and 0 mm, respectively (Figure 7). The highest average value of error was observed for the thickness of 0.2 mm and infill of 50%, in disagreement with the other values corresponding to these parameters. On the other hand, the lowest value seen was in the thickness of 0.16 mm and 75 % infill, however, there was no considerable discrepancy among the other values corresponding to the layer thickness of 0.16 mm. Overall, the smallest errors were seen at the 0.16 mm thickness.

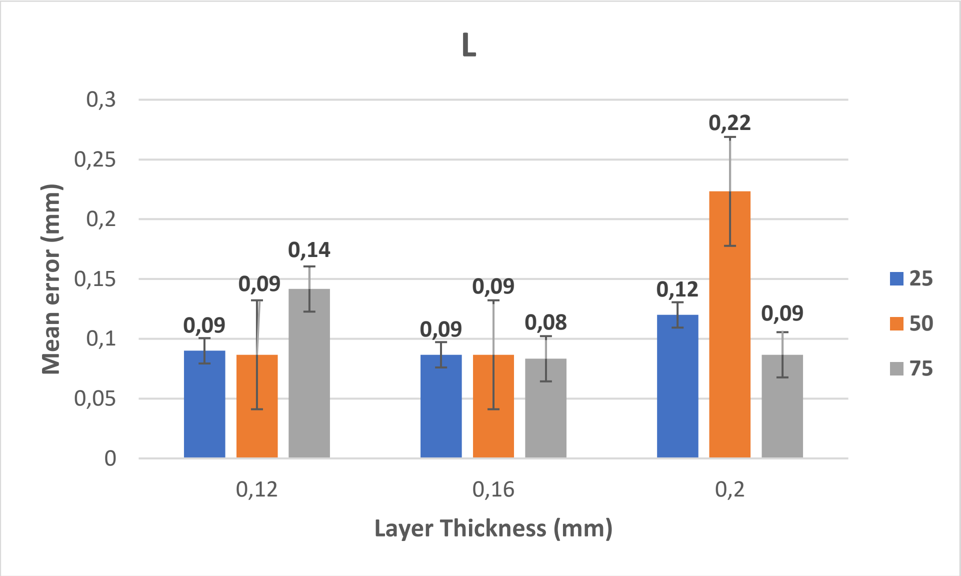

Figure 7. Graph plotted of length error per layer thickness for 25%, 50% and 75% infill respectively

The ANOVA (Table 5) related to the length values shows that the layer thickness and infill density parameters do not significantly impact the length dimensions (Calculated F is smaller than Critical F, not rejecting null hypothesis). The interaction between these two parameters also has no significant impact on this dimension.

Table 5. Length

Source	*SQ*	*DF*	*MQ*	*F*	*Critical F*
Layer thickness	0.030878	2	0.015439	2.006305	5.110318
Infill density	0.011633	2	0.005817	0.755884	5.110318
Factors interaction	0.060756	4	0.015189	1.973817	3.767427
Error	0.346283	45	0.007695		
Total	0.44955	53			

3.2.2 Width

The width errors for the 50% and 75% infill densities increased as the layer thickness parameter increased (Figure 8). An average discrepant value that can be noticed is 0.3 mm, referring to the parameters of 0.2 mm of layer thickness and 75% infill. The most linear growth can be verified for the 50% infill parameter, which presented values of 0.12 mm, 0.18 mm and 0.21 mm of error for the layer thicknesses of 0.12 mm, 0.16 mm and 0.2 mm, respectively.

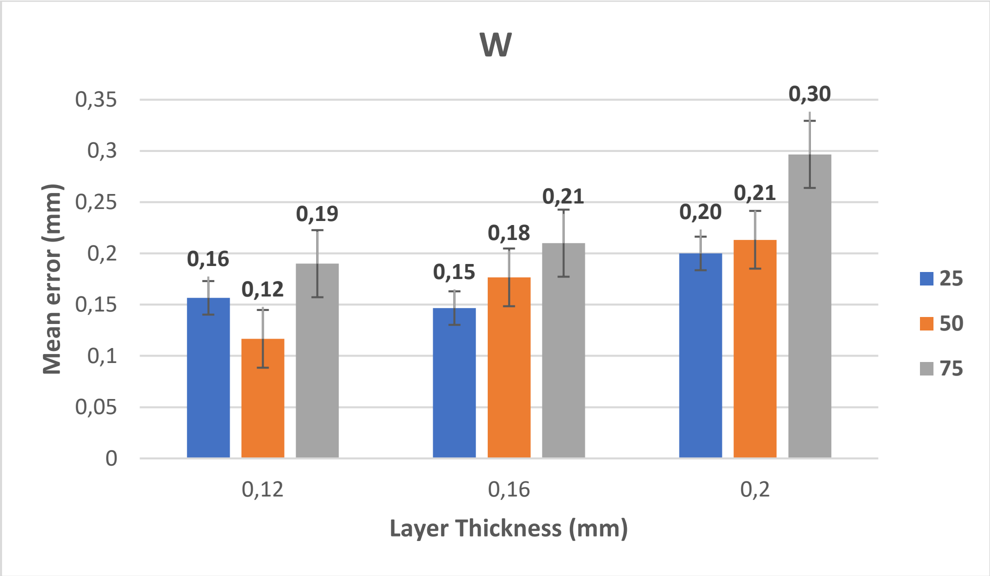

Figure 8. Graph plotted of mean error of width by layer thickness for 25%, 50% and 75% infill density respectively

According to the ANOVA (Table 6) referring to the width values of the specimens, it is noted that both the layer thickness and the infill density impact this dimension. However, the interaction between the parameters does not present a significant action in the width dimension.

Table 6. Width

Source	*SQ*	*DF*	*MQ*	*F*	*Critical F*
Layer thickness	0.064637	2	0.032319	15.21269	5.110318
Infill density	0.048993	2	0.024496	11.53068	5.110318
Factors interaction	0.012163	4	0.003041	1.431311	3.767427
Error	0.0956	45	0.002124		
Total	0.221393	53			

3.2.3 Thickness

Considering the average thickness error graph, it can be seen that the average error value for the layer thicknesses of 0.12 mm and 0.16 mm varies between - 0.17 mm and - 0.19 mm (Figure. 9). Values of mean errors decreased with increasing infill density. The highest error value in each layer thickness is related to the 25% infill.

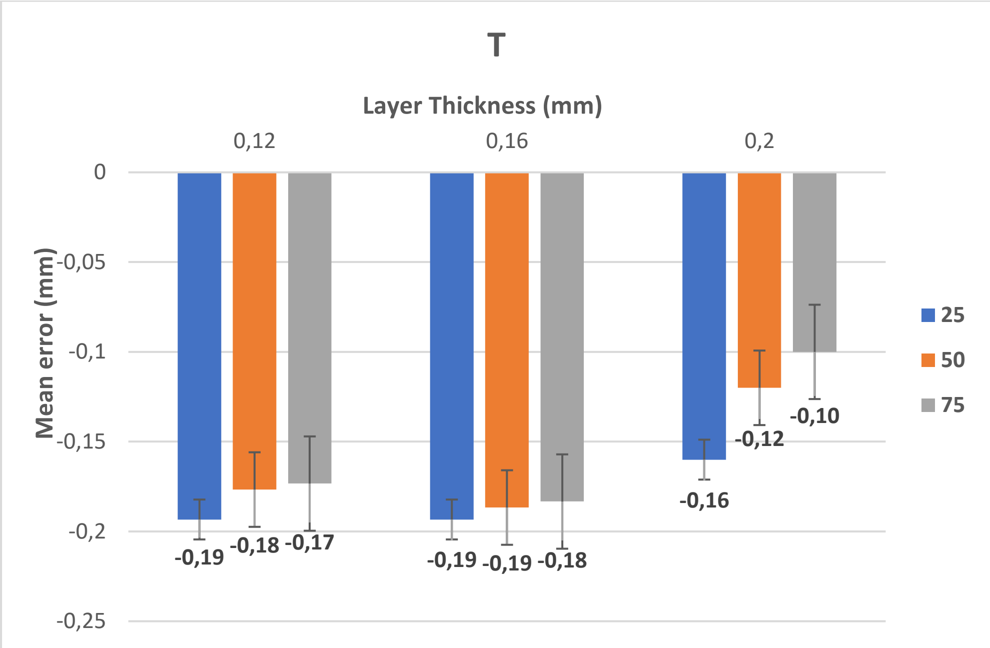

Figure 9. Graph plotted of mean thickness error per layer thickness for 25%, 50% and 75% infill respectively

The ANOVA (Table 7) related to the thickness of the specimen shows that layer thickness is an influential factor in this dimension. The interaction between the parameters does not interfere with the thickness of the specimen.

Table 7. Thickness

Source	*SQ*	*DF*	*MQ*	*F*	*Critical F*
Layer thickness	0.040459	2	0.02023	14.13561	5.110318
Infill density	0.008548	2	0.004274	2.986542	5.110318
Factors interaction	0.004341	4	0.001085	0.758282	3.767427
Error	0.06440	45	0.001431		
Total	0.117748	53			

4. CONCLUSION

The influence of the layer thickness and infill density parameters on the UTS, length, width and thickness dimensions of the specimens made of ePLA-LW of the eSUN brand was investigated. This material is quite versatile in terms of density, which can be controlled by the temperature of the extrusion nozzle. This work investigated the behaviour of this material under conditions where there is still no foaming, at an extrusion temperature of 200°C. The specimens were manufactured by the FDM process by a Creality Ender 3 printer, and the parameters were varied among the 54 printed specimens. After carrying out the tensile tests and measuring the dimensions of the specimens, the following conclusions could be reached:

- Although both parameters influence the UTS of PLA, the infill density plays a major role in this material property;
- Between 0.12 mm, 0.16 mm and 0.2 mm, the layer thickness of 0.16 mm presents higher UTS for ePLA-LW;
- The higher the infill density, the greater the UTS of the ePLA-LW;
- Width is the only dimension affected by both parameters considered;
- The thickness of the ePLA-LW is influenced solely by the layer thickness parameter;
- Body length is not affected by either parameter;

The interaction between the two parameters is not an influential factor in any dimension and also does not affect the UTS of ePLA-LW.

5. ACKNOWLEDGEMENTS

This study was financed in part by the Coordenação de Aperfeiçoamento de Pessoal de Nível Superior – Brasil (CAPES) – Finance Code 001.

6. REFERENCES

Alghamdi, S. S., John, S., Choudhury, N. R., & Dutta, N. K. (2021). Additive manufacturing of polymer materials: Progress, promise and challenges. *Polymers*, *13*(5), 1–39. https://doi.org/10.3390/POLYM13050753

Castelo Branco, R. R., Martins, K. Y. N., Filgueira, A. K. L., Valadares, E. J. O., Galdino, K. E., Morais, M. E. de, Ramos, M. das G. O., Martins, N. do N., Martins, K. Y. N., & Rodrigues, J. K. G. (2021). Caracterização da performance do material Poliácido Lático (PLA) manufaturado pela tecnologia de Modelagem de Fusão e Deposição (FDM). *Research, Society and Development*, *10*(8), e44210817348. https://doi.org/10.33448/rsd-v10i8.17348

Ceulemans et. al. (2020). Patents and additive manufacturing: Trends in 3D printing technologies. *European Patent Office*, 84. https://www.researchgate.net/publication/353637859_Patents_and_additive_manufacturing_Trends_in_3D_printing_technologies

Chacón, J. M., Caminero, M. A., García-Plaza, E., & Núñez, P. J. (2017). Additive manufacturing of PLA structures using fused deposition modelling: Effect of process parameters on mechanical properties and their optimal selection. *Materials & Design*, *124*, 143–157. https://doi.org/10.1016/j.matdes.2017.03.065

Cho, E. E., Hein, H. H., Lynn, Z., Hla, S. J., & Tran, T. (2019). Investigation on Influence of Infill Pattern and Layer Thickness on Mechanical Strength of PLA Material in 3D Printing Technology. *Journal of Engineering and Science Research*, *3*(2), 27–37. https://doi.org/10.26666/rmp.jesr.2019.2.5

Cobos, C. M., Garzón, L., López Martinez, J., Fenollar, O., & Ferrandiz, S. (2019). Study of thermal and rheological properties of PLA loaded with carbon and halloysite nanotubes for additive manufacturing. *Rapid Prototyping Journal*, *25*(4), 738–743. https://doi.org/10.1108/RPJ-11-2018-0289/FULL/XML

Durakovic, B. (2018). Design for additive manufacturing: Benefits, trends and challenges. *Periodicals of Engineering and Natural Sciences (PEN)*, *6*(2), 179–191. https://doi.org/10.21533/PEN.V6I2.224

ESUN. (2022). *ePLA-LW - eSUN 3D Printing Materials*. EPLA-LW. https://www.esun3d.com/epla-lw-product/

Fernandes, J. F. M., (n.d.) Study of the Influence of 3D Printing Parameters on the Mechanical Properties of PLA. Instituto Superior Técnico, Universidade de Lisboa. https://www.google.com/url?sa=i&url=https%3A%2F%2Ffenix.tecnico.ulisboa.pt%2FdownloadFile%2F281870113703682%2FExtended%2520Abstract_73521.pdf&psig=AOvVaw0xd-apCpcCQEv_1nV80mQQ&ust=1677933688377000&source=images&cd=vfe&ved=0CBAQjhxqFwoTCLDZgqrkv_0CFQAAAAAdAAAAABAE

Gendviliene, I., Simoliunas, E., Rekstyte, S., Malinauskas, M., Zaleckas, L., Jegelevicius, D., Bukelskiene, V., & Rutkunas, V. (2020). Assessment of the morphology and dimensional accuracy of 3D printed PLA and PLA/HAp scaffolds. *Journal of the Mechanical Behavior of Biomedical Materials*, *104*, 103616. https://doi.org/10.1016/j.jmbbm.2020.103616

Goh, G. D., Agarwala, S., Goh, G. L., Dikshit, V., Sing, S. L., & Yeong, W. Y. (2017). Additive manufacturing in unmanned aerial vehicles (UAVs): Challenges and potential. *Aerospace Science and Technology*, *63*(December), 140–151. https://doi.org/10.1016/j.ast.2016.12.019

Hanon, M. M., Marczis, R., & Zsidai, L. (2019). Anisotropy Evaluation of Different Raster Directions, Spatial Orientations, and Fill Percentage of 3D Printed PETG Tensile Test Specimens. *Key Engineering Materials*, *821*, 167–173. https://doi.org/10.4028/www.scientific.net/KEM.821.167

Hanon, M. M., Marczis, R., & Zsidai, L. (2020). Influence of the 3D Printing Process Settings on Tensile Strength of PLA and HT-PLA. *Periodica Polytechnica Mechanical Engineering*, *65*(1), 38–46. https://doi.org/10.3311/PPme.13683

Hanon, M. M., Zsidai, L., & Ma, Q. (2021). Accuracy investigation of 3D printed PLA with various process parameters and different colors. *Materials Today: Proceedings*, *42*, 3089–3096. https://doi.org/10.1016/j.matpr.2020.12.1246

Kafle, A., Luis, E., Silwal, R., Pan, H. M., Shrestha, P. L., & Bastola, A. K. (2021). 3D/4D Printing of Polymers: Fused Deposition Modelling (FDM), Selective Laser Sintering (SLS), and Stereolithography (SLA). *Polymers*, *13*(18), 3101. https://doi.org/10.3390/polym13183101

Kuznetsov, V., Solonin, A., Urzhumtsev, O., Schilling, R., & Tavitov, A. (2018). Strength of PLA Components Fabricated with Fused Deposition Technology Using a Desktop 3D Printer as a Function of Geometrical Parameters of the Process. *Polymers*, *10*(3), 313. https://doi.org/10.3390/polym10030313

Montgomery, D. C., & Runger, G. C. (2018). Tests of Hypotheses for a Single Sample. In *Applied Statistics and Probability for Engineers* (7th ed.). John Wiley & Sons, Inc. https://www.wiley.com/en-us/Applied+Statistics+and+Probability+for+Engineers%2C+7th+Edition-p-9781119400363

Moradi, M., Aminzadeh, A., Rahmatabadi, D., & Hakimi, A. (2021). Experimental investigation on mechanical characterization of 3D printed PLA produced by fused deposition modeling (FDM). *Materials Research Express*, *8*(3), 035304. https://doi.org/10.1088/2053-1591/abe8f3

Nofar, M., & Park, C. B. (2014). Poly (lactic acid) foaming. *Progress in Polymer Science*, *39*(10), 1721–1741. https://doi.org/10.1016/j.progpolymsci.2014.04.001

Pandzic, A., Hodzic, D., & Milovanovic, A. (2019). Effect of infill type and density on tensile properties of pla material for fdm process. Annals of DAAAM and Proceedings of the International DAAAM Symposium, 545–554. https://doi.org/10.2507/30TH.DAAAM.PROCEEDINGS.074

Srinivasan, R., Prathap, P., Raj, A., Kannan, S. A., & Deepak, V. (2020). Influence of fused deposition modeling process parameters on the mechanical properties of PETG parts. *Materials Today: Proceedings*, *27*(xxxx), 1877–1883. https://doi.org/10.1016/j.matpr.2020.03.809

Standau, T., Zhao, C., Murillo Castellón, S., Bonten, C., & Altstädt, V. (2019). Chemical Modification and Foam Processing of Polylactide (PLA). *Polymers, 11*(2), 306. https://doi.org/10.3390/polym11020306

Ultimaker Cura: Powerful, easy-to-use 3D printing software. (n.d.). Retrieved June 20, 2022, from https://ultimaker.com/software/ultimaker-cura

7. RESPONSIBILITY NOTICE

The authors are the only responsible for the printed material included in this paper.